

# A scalable quantum computer with ions in an array of microtraps

J. I. Cirac & P. Zoller

Institute for Theoretical Physics, University of Innsbruck, Austria

Quantum computers require the storage of quantum information in a set of two-level systems (called qubits), the processing of this information using quantum gates and a means of final readout<sup>1</sup>. So far, only a few systems have been identified as potentially viable quantum computer models—accurate quantum control of the coherent evolution is required in order to realize gate operations, while at the same time decoherence must be avoided. Examples include quantum optical systems (such as those utilizing trapped ions<sup>2–9</sup> or neutral atoms<sup>10–12</sup>, cavity quantum electrodynamics<sup>13–15</sup> and nuclear magnetic resonance<sup>16,17</sup>) and solid state systems (using nuclear spins<sup>18</sup>, quantum dots<sup>19</sup> and Josephson junctions<sup>20</sup>). The most advanced candidates are the quantum optical and nuclear magnetic resonance systems, and we expect that they will allow quantum computing with about ten qubits within the next few years. This is still far from the numbers required for useful applications: for example, the factorization of a 200-digit number requires about 3,500 qubits<sup>21</sup>, rising to 100,000 if error correction<sup>22</sup> is implemented. Scalability of proposed quantum computer architectures to many qubits is thus of central importance. Here we propose a model for an ion trap quantum computer that combines scalability (a feature usually associated with solid state proposals) with the advantages of quantum optical systems (in particular, quantum control and long decoherence times).

Our model considers ions stored in an array of microtraps<sup>23</sup> which can be realized by electric and/or laser fields (see Fig. 1). Long-lived internal states of the ions carry the qubits. The main idea is to apply an external field to a particular ion such that its motional wave packet is displaced by a small amount depending on the internal state, analogous to the splitting of the atomic wave packet in atom interferometry. By addressing two neighbouring ions, a differential energy shift due to the Coulomb interaction can be induced, conditional on the state of the two qubits. This implements the two-qubit phase gate required for quantum computation. We emphasize that this mechanism differs fundamentally from our proposal for a quantum computer with trapped ions in a linear trap<sup>2</sup>. In that case, the two-qubit gate was based on the exchange of phonons corresponding to the collective centre-of-mass motion of the ions, which initially had to be cooled to zero temperature. In contrast, in our present proposal the motion of the ions is manipulated independently and there is no zero-temperature requirement. This makes the scheme conceptually simpler and obviously scalable.

We first explain qualitatively the operation of our model system, followed by a quantitative analysis of the requirements. We consider a set of  $N$  ions confined in independent harmonic potential wells which are separated by some constant distance  $d$  (Fig. 1). For simplicity we assume for the moment that each ion is in the ground state of the corresponding potential. We will assume that  $d$  is large enough so that: (1) the Coulomb repulsion is not able to excite the vibrational state of the ions; and (2) the ions can be individually addressed. Each ion stores a qubit in two internal, long-lived states,  $|0\rangle$  and  $|1\rangle$ . The initialization and readout of the quantum register can easily be performed as described<sup>2</sup>. Initially, the global wavefunction describing the state of the ions can be factorized into the one corresponding to their internal state and the one corresponding to their motional state. Single-qubit operations on a given ion can be performed by directing a laser beam with the appropriate intensity and phase to the corresponding ion in such a

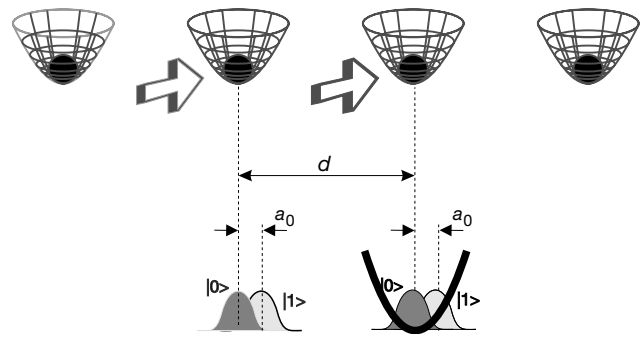


**Figure 1** Schematic setup. Ions are trapped in independent traps. For the gate they are pushed provided they are in state  $|1\rangle$ .

way that its motional state is not affected. Two-qubit gates between two neighbouring ions can be performed by slightly displacing them for a short time  $T$  if they are in a particular internal state, say  $|1\rangle$ . In that case, and provided the ions come back to their original motional state after being pushed, the Coulomb interaction will provide the internal wavefunction (quantum register) with different phases depending on the internal states of the ions. Choosing the time appropriately, the complete process will give rise to the two-qubit gate

$$\begin{aligned} |0\rangle_i |0\rangle_{i+1} |\Psi_{00}\rangle_{\text{rest}} &\rightarrow |0\rangle_i |0\rangle_{i+1} |\Psi_{00}\rangle_{\text{rest}} \\ |0\rangle_i |1\rangle_{i+1} |\Psi_{01}\rangle_{\text{rest}} &\rightarrow |0\rangle_i |1\rangle_{i+1} |\Psi_{01}\rangle_{\text{rest}} \\ |1\rangle_i |0\rangle_{i+1} |\Psi_{10}\rangle_{\text{rest}} &\rightarrow |1\rangle_i |0\rangle_{i+1} |\Psi_{10}\rangle_{\text{rest}} \\ |1\rangle_i |1\rangle_{i+1} |\Psi_{11}\rangle_{\text{rest}} &\rightarrow e^{i\phi} |1\rangle_i |1\rangle_{i+1} |\Psi_{11}\rangle_{\text{rest}} \end{aligned} \quad (1)$$

and in particular, for  $\phi = \pi$ , we have a phase gate. In general, there will be phase factors  $e^{i\phi_i}$  with  $i = 1, \dots, 4$  in each line on the right-hand side of equation (1). There is a global phase and (trivial) single particle phases (such as kinetic phases) which can be undone by single-bit operations leaving us with  $\phi = \phi_4 - \phi_2 - \phi_3 + \phi_1$ . The  $\Psi$  symbols denote the internal state of the rest of the ions, and (where we have not written explicitly) the motional state, because it is factorized out at the beginning and at the end of the gate.

To analyse the operating conditions of this scheme in a more quantitative way, we consider two ions 1 and 2 of mass  $m$  confined by two harmonic traps of frequency  $\omega$  in one dimension (see Fig. 1). The generalization of our analysis to three dimensions and  $N$  ions is straightforward. We denote by  $\hat{x}_{1,2}$  the position operators of the two ions. Now, let us assume that if the ions are in state  $|1\rangle$  in addition to the trap, then the  $i$ th ion is pushed by a force  $F_i(t) = \frac{1}{2} f_i(t) \hbar \omega / a_0$ , where  $f_i(t)$  is some smooth function of time with  $a_0 = (\hbar / 2m\omega)^{1/2}$  the size of the trap ground state. We will take  $f_i(t)$  going from 0 to approximately 1 and then back to 0 as time goes from 0 to  $T$ . The effect of the force is to shift the centre of the harmonic potential to the position  $\bar{x}_i(t) = f_i(t) a_0$ . The corresponding potential is

$$V = \sum_{i=1,2} \frac{1}{2} m \omega^2 (\hat{x}_i - \bar{x}_i(t) |1\rangle_i \langle 1|)^2 + \frac{e^2}{4\pi\epsilon_0} \frac{1}{|d + \hat{x}_2 - \hat{x}_1|} \quad (2)$$

The minimum of the potential determines the equilibrium position of the two ions  $x_{1,2}^{(0)}$  in the absence of the force  $F_i(t)$ ; we can expand the potential around these equilibrium values, where we conveniently redefine the position of the ions as the displacement around these equilibrium values:  $\hat{x}_{1,2} \rightarrow x_{1,2}^{(0)} + \hat{x}_{1,2}$  and  $d \rightarrow d + x_2^{(0)} - x_1^{(0)}$ . We are interested in the limit where (1)  $|\hat{x}_{1,2}| \ll d$  and (2)  $\epsilon |\hat{x}_1 \hat{x}_2| / a_0^2 \ll 1$ , with  $\epsilon$  the ratio of the Coulomb energy,  $e^2 / (4\pi\epsilon_0 d)$ , and the energy of the second ion with respect to the first trap,  $\frac{1}{2} m \omega^2 d^2$ . Furthermore, we assume that the motional state of the pushed ions will change adiabatically with the potential, which, away from  $\epsilon^2 \ll 1$ , requires

$|\dot{f}_i(t)| \ll \omega$ . Expansion of the Coulomb term in powers of  $\hat{x}_{1,2}/d$  gives rise to a term,  $-m\omega^2 \hat{x}_1 \hat{x}_2$ , in equation (2). It is this term which is responsible for entangling the atoms according to equation (1), giving rise to a conditional phase shift

$$\phi = -\frac{1}{2}\epsilon\omega \int_0^T dt f_1(t)f_2(t) \quad (3)$$

if and only if the internal state of both ions is  $|1\rangle$ . Equation (3) can simply be interpreted as arising from the energy shifts due to the Coulomb interactions of atoms accumulated on different trajectories according to their internal states

$$\phi = -\frac{e^2}{4\pi\epsilon_0} \int_0^T dt \left[ \frac{1}{d + \bar{x}_2 - \bar{x}_1} - \frac{1}{d + \bar{x}_2} - \frac{1}{d - \bar{x}_1} + \frac{1}{d} \right],$$

where the four terms are due to atoms in  $|1\rangle_1|1\rangle_2$ ,  $|1\rangle_1|0\rangle_2$ ,  $|0\rangle_1|1\rangle_2$  and  $|0\rangle_1|0\rangle_2$ , respectively. In summary, by selecting the time of the gate  $T \approx 2\pi/(\epsilon\omega)$  (that is,  $\phi = \pi$ ) we have the phase gate, equation (1). We emphasize that equation (3) depends only on mean displacement of the atomic wavepacket and is thus insensitive to the temperature (the width of the wave packet), which will appear in the problem only in higher orders of  $x_{1,2}/d$  of our expansion of equation (2), or in cases of non-adiabaticity. Finally, although we have considered here an adiabatic displacement of the trap centre, similar schemes are possible which are based on time-dependent potentials. As an example, in Table 1 we give the values of the relevant parameters of the problem for the case of Ca, at several trapping frequencies.

We now discuss briefly some of the more technical aspects for some physical realizations of the trapping and state-dependent pushing required in our scheme. Regarding trapping, recent developments in nanofabrication techniques allow us to create arrays of electric or magnetic microtraps<sup>23</sup>. Alternatively, we can first confine the particles with standard ion traps and then switch on an (additional) off-resonant optical lattice potential so that the ions are confined at the bottom of nonconsecutive wells. For example, with CO<sub>2</sub> lasers, very long confinement times can be obtained (of the order of minutes) without having spontaneous emission, and trap frequencies of tens of MHz can be achieved<sup>24</sup>. On the other hand, for the pushing we need a force that acts differently depending on the internal state of the ions. Let us consider one simple possibility, in which  $|1\rangle$  (or  $|0\rangle$ ) corresponds to one of the  $S_{1/2}$  (or  $D_{5/2}$ ) levels, as in Ca, for example (another possibility is to use the method given in ref. 10). A laser standing wave connecting the states  $S_{1/2}$  with the  $P_{1/2}$ , with a detuning  $\Delta$  and forming some angle  $\theta$  with respect to the vector that connects the ions participating in the gate, can be used. We denote by  $\Omega(t)^2 = f(t)\Omega_0^2$  the square of the Rabi frequency and by  $\eta = ka_0\cos(\theta)$  the Lamb–Dicke parameter, where  $k$  is the laser wavevector. Choosing  $\eta\Omega_0^2/(2\Delta) = \omega$  one achieves the required force  $F_i(t) = \frac{1}{2}f_i(t)\hbar\omega/a_0$ . On the other hand, the spontaneous emission rate is reduced by a factor  $r_f = \Omega_0^2/(2\Delta)^2 \ll 1$  (that is,  $\Gamma_{\text{eff}} = r_f\Gamma$ ). We thus obtain the detunings and Rabi frequencies required:  $\Delta = r_f\omega/\eta$  and  $\Omega_0 = r_f^{1/2}\omega/\eta$ . For a 10-MHz trap frequency with  $\eta = 0.1$ , we can choose a reduction factor of  $10^{-4}$  (or  $10^{-6}$ ) by taking  $\Delta = 10^3$  GHz (or  $10^5$  GHz) and  $\Omega_0 = 10$  GHz (or 100 GHz).

**Table 1 Experimental parameters for Ca\***

	$\epsilon = 0.1$			$\epsilon = 0.01$		
$\omega/2\pi$ (MHz)	1	5	20	1	5	20
$d$ ( $\mu\text{m}$ )	12	4	1.6	26	9	3.5
$a_0/d$ ( $\times 10^{-3}$ )	0.9	1.2	1.5	0.4	0.5	0.7
$T$ ( $\mu\text{s}$ )	10	2	0.5	100	20	5

For a given trap frequency  $\omega$  and a (small) parameter  $\epsilon$  we give the distance  $d$  between the ions, size of the trap ground state relative to the distance  $a_0/d$  and time of the gate  $T$ . We have taken two values of  $\epsilon = 0.1$  and  $0.01$  so that the condition  $\epsilon^2 \ll 1$  is well satisfied. The other requirement  $a_0/d \ll 1$  is also clearly fulfilled. The distance between the ions and the corresponding gate times are also displayed. We note that independent traps permits high trap frequencies and therefore short operation times, which presents obvious advantages for avoiding decoherence.

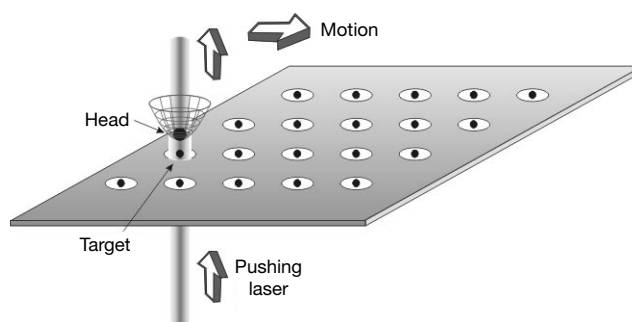


**Figure 2** Scalable quantum computer. We envisage a two-dimensional array of independent ion traps<sup>23</sup>, and a different ion (Head) that moves above this plane, approaching any particular ion. By switching on a laser propagating in the perpendicular direction to the plane, we can perform the two-qubit gate between the target ion and the head as explained above. In particular, we can swap the state of that ion to the head, which immediately allows us to perform entanglement operations between distant ions.

A possible quantum computer model based on the ideas presented above is outlined in Fig. 2. This scheme has several attractive features: (1) The head and the target can be brought very close together, since we do not have to address them independently. This implies that the gate operation time can be greatly decreased. (2) The distance between the ions in the plane can be very large, since no interaction between them is required. (3) We can think of having several heads running in parallel. (4) We may use a different isotope or ion species for the head, which facilitates the independent motion of the head. (5) The two-dimensional structure facilitates scaling up to a larger number of qubits.

A possible experimental realization of the scalable quantum computer model will represent significant experimental challenges. First, one has to create arrays of microtraps and load them with ions. According to ref. 23, a possible way of doing that is to use elliptical traps, which can be constructed from a single flat electrode, yielding a device that is simpler, smaller and stronger than a linear trap, and is suitable for microfabrication in large arrays. Second, decoherence must be avoided. There are several sources of decoherence in the present model. For example, the motional states of the ions can get entangled with the environment. This is relevant, however, only during the gate operations, and not during the time in which the head is moved (because the internal state of the ions is factorized from the motional degrees of freedom)—provided, of course, that the heating rate is not too high. On the other hand, the time for the gate operation in our scheme (which is only limited by the trapping frequency) can be much smaller than the typical decoherence times reported in experiments with microtraps (ref. 9 and references therein). Finally, laser intensity fluctuations of the pushing laser must be controlled in order to avoid dephasings.

We have here proposed a new scheme to perform quantum computations with trapped ions. Despite being conceptually simple, we believe that the scheme is within reach of present experimental technologies. In particular, our two-dimensional array setup offers an experimental avenue towards reaching a scalable quantum computer. Finally, we would like to stress that apart from using it for quantum computations, our scheme can emulate Ising (and similar) models<sup>25</sup> with adjustable parameters simply by leaving on all the pushing lasers which are responsible for effective spin–spin interaction. □

Received 16 November 1999; accepted 16 February 2000.

- DiVincenzo, D. P. Two-bit gates are universal for quantum computation. *Phys. Rev. A* **51**, 1015–1022 (1995).
- Cirac, J. I. & Zoller, P. Quantum computations with cold trapped ions. *Phys. Rev. Lett.* **74**, 4091–4094 (1995).
- Monroe, C., Meekhof, D. M., King, B. E., Itano, W. M. & Wineland, D. J. Demonstration of a fundamental quantum logic gate. *Phys. Rev. Lett.* **75**, 4714–4717 (1995).

4. Poyatos, J. F., Cirac, J. I. & Zoller, P. Quantum gates with hot trapped ions. *Phys. Rev. Lett.* **81**, 1322–1325 (1998).
5. Steane, A. The ion trap quantum information processor. *Appl. Phys. B* **64**, 623–642 (1997).
6. Turchette, Q. A. *et al.* Deterministic entanglement of two trapped ions. *Phys. Rev. Lett.* **81**, 3631–3634 (1998).
7. Roos, Ch. *et al.* Quantum state engineering on an optical transition and decoherence in a Paul trap. Pre-print quant-ph/9909038 at (xxx.lanl.gov) (1999).
8. Sorensen, A. & Molmer, K. Quantum computation with ions in thermal motion. *Phys. Rev. Lett.* **82**, 1971–1974 (1999).
9. Wineland, D. J. *et al.* Experimental issues in coherent quantum-state manipulation of trapped atomic ions. *J. Res. Natl Inst. Stand. Technol.* **103**, 259 (1998).
10. Jaksch, D., Briegel, H.-J., Cirac, J. I., Gardiner, C. W. & Zoller, P. Entanglement of atoms via cold controlled collisions. *Phys. Rev. Lett.* **82**, 1975–1978 (1999).
11. Brennen, G. K., Caves, C. M., Jessen, P. S. & Deutsch, I. H. Quantum logic gates in optical lattices. *Phys. Rev. Lett.* **82**, 1060–1063 (1999).
12. Calarco, T. *et al.* Quantum gates with neutral atoms: Controlling collisional interactions in time dependent traps. Pre-print quant-ph/9905013 at (xxx.lanl.gov) (1999).
13. Pellizzari, T., Gardiner, S. A., Cirac, J. I. & Zoller, P. Decoherence, continuous observation, and quantum computing: a cavity QED model. *Phys. Rev. Lett.* **75**, 3788–3791 (1995).
14. Turchette, Q. A., Hood, C. J., Lange, W., Mabuchi, H. & Kimble, H. J. Measurement of conditional phase shifts for quantum logic. *Phys. Rev. Lett.* **75**, 4710–4713 (1995).
15. Maître, X. *et al.* Quantum memory with a single photon in a cavity. *Phys. Rev. Lett.* **79**, 769–772 (1997).
16. Cory, D. G., Fahmy, A. F. & Havel, T. F. Ensemble quantum computing by NMR spectroscopy. *Proc. Natl Acad. Sci. USA* **94**, 1634–1639 (1997).
17. Gershenfeld, N. A. & Chuang, I. L. Bulk spin-resonance quantum computation. *Science* **275**, 350–356 (1997).
18. Kane, B. E. A silicon-based nuclear spin quantum computer. *Nature* **393**, 133–137 (1998).
19. Loss, D. & DiVincenzo, D. P. Quantum computation with quantum dots. *Phys. Rev. A* **57**, 120–126 (1998).
20. Makhlin, Y. & Schön, G. Josephson-junction qubits with controlled couplings. *Nature* **398**, 305–307 (1999).
21. Beckman, D., Chari, A. N., Devabhaktuni, S. & Preskill, J. Efficient networks for quantum factoring. *Phys. Rev. A* **54**, 1034–1063 (1996).
22. Steane, A. M. Efficient fault-tolerant quantum computing. Pre-print quant-ph/9809054 at (xxx.lanl.gov) (1998).
23. DeVoe, R. G. Elliptical ion traps and trap arrays for quantum computation. *Phys. Rev. A* **58**, 910–914 (1998).
24. Friebe, S., D'Andrea, C., Walz, J., Weitz, M. & Hänsch, T. W. CO<sub>2</sub> laser optical lattice with cold rubidium atoms. *Phys. Rev. A* **57**, R20–R23 (1998).
25. Lloyd, S. Universal quantum simulators. *Science* **273**, 1073–1078 (1996).

#### Acknowledgements

We thank R. Blatt, D. Leibfried and D. Wineland for comments. This work was supported by the Austria Science Foundation, TMR networks from the European Community, and the Institute for Quantum Information GmbH.

Correspondence and requests for materials should be addressed to P.Z.  
(e-mail: peter.zoller@uibk.ac.at).

## Magnetoresistance from quantum interference effects in ferromagnets

N. Manyala\*, Y. Sidis\*†, J. F. DiTusa\*, G. Aeppli‡, D.P. Young§ & Z. Fisk§

\* Department of Physics and Astronomy, Louisiana State University, Baton Rouge, Louisiana 70803, USA

† NEC, 4 Independence Way, Princeton, New Jersey 08540, USA

§ National High Magnetic Field Facility, Florida State University, Tallahassee, Florida 32306, USA

The desire to maximize the sensitivity of read/write heads (and thus the information density) of magnetic storage devices has stimulated interest in the discovery and design of new magnetic materials exhibiting magnetoresistance. Recent discoveries include the 'colossal' magnetoresistance in the manganites<sup>1–4</sup> and the enhanced magnetoresistance in low-carrier-density ferromagnets<sup>4–6</sup>. An important feature of these systems is that the electrons involved in electrical conduction are different from those responsible for the magnetism. The latter are localized

and act as scattering sites for the mobile electrons, and it is the field tuning of the scattering strength that ultimately gives rise to the observed magnetoresistance. Here we argue that magnetoresistance can arise by a different mechanism in certain ferromagnets—quantum interference effects rather than simple scattering. The ferromagnets in question are disordered, low-carrier-density magnets where the same electrons are responsible for both the magnetic properties and electrical conduction. The resulting magnetoresistance is positive (that is, the resistance increases in response to an applied magnetic field) and only weakly temperature-dependent below the Curie point.

The oxides of manganese that are known to have high magnetoresistance are derived from chemical doping of insulators that are also magnetically ordered. Thus, the local moments that are ordered in the doped materials already exist in the insulator, with the result that, to a first approximation, metallicity and magnetism are independent properties<sup>6</sup>. The electrical resistance is reduced when there is less scattering of the conduction electrons by the spins of the localized electrons. To the extent that an external field reduces the disorder among the local spins, the scattering will be reduced, resulting in a negative magnetoresistance. When searching for different mechanisms for magnetoresistance, we need to consider compounds where the insulating parent is non-magnetic. In addition, the parent should have strong electron–electron interactions so that magnetism appears readily upon doping. Insulators which satisfy this criterion are referred to as strongly correlated, or Kondo insulators<sup>7</sup>. A particularly simple Kondo insulator is FeSi, which has attracted attention for over 30 years because of its anomalous temperature-dependent electrical, optical and magnetic properties<sup>7–11</sup>. Previous investigations reveal a metal–insulator transition with either Al substitution for Si (hole doping) or Co substitution for Fe (electron doping) at the level of 1% (refs 12 and 13). The transition is very similar to that found in classic semiconductors such as phosphorus-doped silicon or antimony-doped germanium, except that the effective masses of the holes (electrons) are much larger. FeSi is isostructural (cubic B-20) and continuously miscible with the classic metallic ferromagnet MnSi (see, for example, ref. 14) and the diamagnetic metal CoSi (ref. 8); it is therefore possible to control the carrier sign—positive (holes) for substitution of Mn for Fe and negative (electrons) for substitution of Co—and the density throughout a magnetically interesting phase diagram, shown in Fig. 1. Modest (20%) dilution of Mn by Fe destroys the ferromagnetism of MnSi while retaining metallicity. In contrast, the alloy Fe<sub>1–y</sub>Co<sub>y</sub>Si is remarkable in that although the two end members ( $y = 0$ ) and ( $y = 1$ ) are both non-magnetic, it is magnetic for almost all intermediate compositions<sup>8,15,16,17</sup>. This is the alloy that displays unusual magnetoresistance, clearly distinguishable from that found in more ordinary magnets such as MnSi.

Our samples were either polycrystalline pellets or small single crystals grown from Sb and Sn fluxes. We produced polycrystalline samples from high purity starting materials by arc melting in an argon atmosphere. To improve homogeneity, the Fe<sub>1–y</sub>Co<sub>y</sub>Si (Fe<sub>1–x</sub>Mn<sub>x</sub>Si) samples were annealed for 24 hours at 1,200 °C (four days at 1,000 °C) in evacuated quartz ampoules. Powder X-ray spectra showed all samples to be single phase with a lattice constant that is linearly dependent on Co and Mn concentration. The linearity demonstrates that Co or Mn successfully replaces Fe over the entire concentration range ( $0 \leq x \leq 1$ ;  $0 \leq y \leq 1$ ). Energy dispersive X-ray microanalysis yielded results consistent with the nominal concentrations. The Hall effect data establish the sign and density of the carriers in our samples and demonstrate a systematic increase in carrier density ( $n$ ) proportional to the Co and Mn concentration at small  $x$  and  $y$ . They clearly show the existence of a metallic state in the concentration range studied ( $0.03 \leq x \leq 1$ ;  $0.05 \leq y \leq 0.30$ ), with only a small variation of  $n$  with temperature ( $T$ ). In particular,  $n$  does not appear to change as the Curie temperature ( $T_C$ ) is traversed.

† Present address: Laboratoire Léon Brillouin, CEA-CNRS, CE Saclay, 91191 Gif-Sur-Yvette, France.